



## Intermolecular Interactions between TNAZ and H<sub>2</sub>O: a DFT Study

Mohsen OFTADEH<sup>1,\*</sup>, Shahryar SELAHVARZI<sup>1</sup>  
and Mohammad Hossein KESHAVARZ<sup>2</sup>

<sup>1</sup>Chemistry Department, Payame Noor University,  
19395-4697 Tehran, I. R. Iran

<sup>2</sup>Department of Chemistry, Malek-ashtar University of Technology,  
Shahin-shahr, P.O. Box 83145/115, I. R. Iran

\*E-mail: [m\\_oftadeh@pnu.ac.ir](mailto:m_oftadeh@pnu.ac.ir)

**Abstract:** All of the possible TNAZ/H<sub>2</sub>O complexes (**1**, **2** and **3**), as well as the uncomplexed form, were fully optimized with the density functional method. Complex **3** was the most stable, with the largest corrected intermolecular interaction energy. Charge redistribution mainly occurs on the adjacent N–O...H atoms of the submolecules. Strong hydrogen bonds predominantly contribute to the interaction energies. It is energetically and thermodynamically unfavourable for TNAZ to bind with H<sub>2</sub>O and to form any stable complexes at room temperature.

**Keywords:** 1,3,3-trinitroazetidine (TNAZ)/H<sub>2</sub>O complex, intermolecular interaction, DFT, natural bond orbital, thermodynamic properties

## Introduction

1,3,3-Trinitroazetidine (TNAZ) (Figure 1) is a high performance, melt castable explosive that has been proposed as a potential replacement for TNT [1]. The low melting point of TNAZ enables processing of its formulations on modified production lines, whilst its performance is approximately 30% greater than TNT. It has also been reported that TNAZ is a highly energetic material, more powerful than RDX, and less sensitive than most other nitramines [2]. Furthermore, TNAZ has many added advantages over known explosives. TNAZ is a white crystalline material, crystallised from chloroform [3].

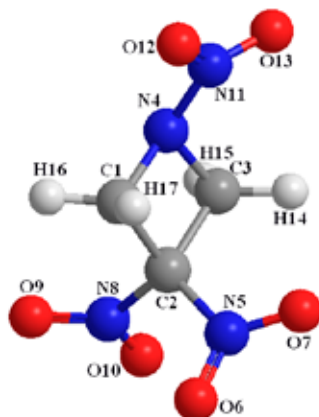


**Figure 1.** Optimized structure of TNAZ.

TNAZ has a density of  $1.85 \text{ g/cm}^3$  (confirmed by X-ray crystallography), which further indicates the stability of the dense material [3, 4]. It has excess oxygen available for the oxidation of fuel ingredients and has only half the impact sensitivity of HMX, meaning that it can sustain twice the energy of impact as HMX without detonating. Unlike HMX, TNAZ is soluble in molten TNT, and is compatible with aluminium, steel, brass and glass. Furthermore, it is not hygroscopic and does not pose problems from a processing view point. TNAZ is a high-energy molecule with two energetic functional groups, *i.e.*, C–NO<sub>2</sub> and N–NO<sub>2</sub>, representing two active sites for its decomposition. It is a strained-ring energetic material with a melting point of 101 °C and has good thermal stability up to 240 °C. It may be safely concluded that TNAZ is a steam-castable material, which is attractive as an explosive or as a candidate component for explosives/propellants with low sensitivity, good stability and enhanced performance over existing military formulations [5].

The hygroscopicity or sensitivity to moisture is one of the many physical properties of explosives and igniters. Knowledge of the effect of a moist atmosphere is of interest to persons dealing with explosives. There are many variables affecting the amount of moisture which will be adsorbed by solid substances. This depends, among other things, upon unsaturated forces on the surface of the crystalline lattice of the substance [6]. It is possible that TNAZ could come into contact with water during manufacture or could absorb water during storage; this absorption of moisture relates to the interaction between TNAZ and water. Consequently, the kinetics of its decomposition and explosive properties such as sensitivity, strength and velocity of detonation will be affected

by the formation of water complexes. Stability is also affected by the presence of moisture since moisture promotes decomposition of the explosive and, in addition, can cause corrosion of the explosive's metal container.

The density functional theory (DFT) method deals with electron correlation but is still computationally economical. By combining Becke's three parameters with Lee-Yang-Parr correlation functions (B3LYP), both the structure and the binding energy have been found to be consistent with experimental data for systems with strong H-bonds [7-9]. Fortunately, a large number of recent calculations have shown that B3LYP can give a good prediction of the energies for nitramines [10, 11].

In a previous study [12], the quantities of the activation barriers, enthalpies, entropies and free energies of a few initial steps in the decomposition pathways of TNAZ and some of its derivatives with -F, -CN and -OCH<sub>3</sub> groups were computed by means of DFT with the B3LYP/6-31G model. For all of the derivatives, the results essentially confirmed that N-NO<sub>2</sub> cleavage is the most convenient pathway in the kinetic and thermodynamic properties of their decomposition.

While TNAZ is not hygroscopic and does not pose problems from a processing view point [5], there is no theoretical or experimental information available about the intermolecular interactions between TNAZ and H<sub>2</sub>O. In this work, we have attempted to evaluate complex formation between TNAZ and water molecules by carrying out DFT calculations at the B3LYP/6-311++G\*\* level in order to obtain the best qualified, predicted and comparable theoretical results with experimental data from the energetic and structural pattern favourable from the complex formation point of view.

### Computational methods

TNAZ, H<sub>2</sub>O and their complexes obtained from Chem3D software were fully optimized at the DFT/B3LYP level by the Berny method [13] with the 6-311++G\*\* basis set. The intermolecular interaction energy was calculated with the zero point energy (ZPE) correction and basis set superposition error (BSSE) correction, which can be checked by the Boys and Bernardi counterpoise procedure (CP) [14]. Natural bond orbital (NBO) analyses and frequency calculations were performed on each optimized structure. NBO analysis was performed to reveal the origin of the interaction. The thermodynamic data and their changes upon complex formation were derived from statistical thermodynamics based on the frequencies. All quantum chemical calculations concerning the gaseous phase were performed with the Gaussian 03 [15] program on a PC equipped with a core i5® processor.

## Results and Discussion

### Optimized geometries

Figure 2 shows the optimized geometries of TNAZ and its complexes with water (**1**, **2**, **3**) at the B3LYP/6-311++G\*\* level. All three complexes possess  $C_1$  symmetry and have only one contacting point. Table 1 summarises the optimized geometry structures of the monomer and three types of complexes. It can be seen that the change in bond length for complex **3** is slightly greater than for complexes **2** and **3**. According to the intermolecular distances and the change in bond length, complex **3** is more stable than complexes **1** and **2**. In contrast to complexes **1** and **2**, the dihedral angles of complex **3** are significantly changed from the TNAZ monomer, with a difference of  $50^\circ$ , which implies that the influence of the interaction on the internal rotation is large. However, variations in the bond angles for all three complexes were small in comparison with TNAZ. This means that the influence of the interaction on bond bending is small.

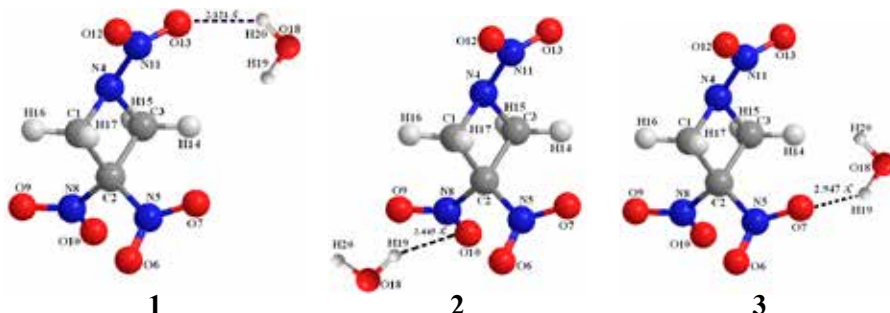


**Figure 2.** Optimized structures of TNAZ/H<sub>2</sub>O complexes **1**, **2**, and **3**.

### NBO charges and charge transfer

The intermolecular NBO interactions that reveal the origin of the intermolecular interactions between donor and acceptor belong to different submolecules in a cluster. The amount of transferred partial charge between a donor and an acceptor species ( $q_{\text{donor} \rightarrow \text{acceptor}}$ ) was calculated by the occupation numbers from the NBO data for evaluating the orbital interaction energy ( $\Delta E^{(2)}$ ) between the HOMO and LUMO of the donor-acceptor system. In a quantitative sense, the energetic effects due to these interactions may be estimated by second-order perturbation, theoretical expressions of the following form [16]:

$$q_{\text{donor} \rightarrow \text{acceptor}} \cong 2 \left[ \frac{\langle \Psi_{\text{don}}^* | \hat{F} | \Psi_{\text{don}} \rangle}{\epsilon_{\text{acc}} - \epsilon_{\text{don}}} \right]^2 \quad (1)$$

$$\Delta E^2 = 2 \frac{\langle \Psi_{\text{don}}^* | \hat{F} | \Psi_{\text{don}}^* \rangle^2}{\epsilon_{\text{acc}} - \epsilon_{\text{don}}} \quad (2)$$

where  $F$  is the Fock operator,  $\langle \Psi_{\text{don}}^* | \hat{F} | \Psi_{\text{don}}^* \rangle$  is the matrix element of the Fock operator between the donor and acceptor wave functions and  $\epsilon_{\text{don}}$  and  $\epsilon_{\text{acc}}$  are the energies of the donor and acceptor orbitals involved in electron transfer.

**Table 1.** Optimized structural properties including bond lengths (Å), bond angles and dihedrals angles of TNAZ, H<sub>2</sub>O, complexes **1**, **2**, and **3** at B3LYP/6-311++G\*\* level

Bond	Monomer	1	2	3	Bond	Monomer	1	2	3
C <sub>1</sub> -C <sub>2</sub> *	1.543	1.544	1.544	1.54	N <sub>5</sub> -O <sub>6</sub>	1.213	1.211	1.212	1.216
C <sub>1</sub> -N <sub>4</sub>	1.481	1.479	1.480	1.482	N <sub>5</sub> -O <sub>7</sub>	1.217	1.217	1.215	1.215
C <sub>1</sub> -H <sub>16</sub>	3.016	3.022	3.020	3.007	N <sub>8</sub> -O <sub>9</sub>	1.214	1.216	1.215	1.216
C <sub>1</sub> -H <sub>17</sub>	2.825	2.830	2.819	2.836	N <sub>8</sub> -O <sub>10</sub>	1.217	1.215	1.218	1.214
C <sub>2</sub> -C <sub>3</sub>	1.540	1.541	1.540	1.543	N <sub>11</sub> -O <sub>12</sub>	1.219	1.219	1.220	1.227
C <sub>2</sub> -N <sub>5</sub>	1.53	1.532	1.531	1.520	N <sub>11</sub> -O <sub>13</sub>	1.219	1.227	1.219	1.220
C <sub>2</sub> -N <sub>8</sub>	1.525	1.523	1.526	1.530	O <sub>18</sub> -H <sub>19</sub>	0.962	0.961	0.964	0.963
C <sub>3</sub> -N <sub>4</sub>	1.482	1.486	1.484	1.480	O <sub>18</sub> -H <sub>20</sub>	0.962	0.966	0.962	0.964
C <sub>3</sub> -H <sub>14</sub>	2.833	2.838	2.817	2.840	O <sub>10</sub> -H <sub>19</sub>	-	0.705	0.245	0.574
C <sub>3</sub> -H <sub>15</sub>	3.010	3.013	3.019	2.994	O <sub>7</sub> -H <sub>19</sub>	-	0.632	0.397	0.295
N <sub>4</sub> -N <sub>11</sub>	1.396	1.382	1.394	1.388	O <sub>13</sub> -H <sub>19</sub>	-	0.372	0.577	0.405
Bond angle					Dihedral angle				
3.2.1	89.48	87.51	89.37	89.58	4-1-2-3	9.33	-2.40	10.04	-7.69
4.1.2	87.33	89.10	87.39	87.54	5-2-1-4	128.14	117.78	128.12	127.60
5.2.1	113.91	113.66	114.38	114.97	6-5-2-1	105.09	89.08	124.45	54.60
6.5.2	117.25	118.54	118.19	115.05	7-5-2-1	-71.71	-88.88	-53.99	-125.34
7.5.2	115.47	116.80	114.59	117.81	8-2-1-4	-107.23	-112.45	-107.76	-107.64
8.2.1	116.05	114.41	114.54	115.48	9-8-2-1	-22.03	-16.31	-36.64	28.39
9.8.2	117.76	117.66	116.57	115.69	10-8-2-1	157.74	162.37	143.75	-154.89
10.8.2	114.98	117.30	116.85	117.20	11-4-1-2	-137.12	-130.40	-137.81	-134.96
11.4.1	119.44	119.83	119.26	119.83	12-11-4-1	-33.56	-32.95	-33.48	-31.84
12.11.4	116.05	117.59	116.13	116.43	13-11-4-1	149.02	151.78	149.18	150.83
13.11.4	116.05	117.85	116.16	116.25	14-3-2-1	-125.49	-114.46	-126.48	-123.49
14.1.4	113.16	116.62	112.99	113.20	15-3-2-1	104.85	116.67	104.54	106.46
15.1.4	114.68	110.20	114.81	113.64	16-1-4-11	-22.56	-12.20	-23.97	-21.46
16.3.2	115.82	114.71	115.83	116.37	17-1-4-11	106.41	114.01	105.08	108.19
17.3.2	112.71	114.74	112.71	112.23					

\* Atomic numbering from 1 to 17 belongs to TNAZ and that from 18 to 20 belongs to H<sub>2</sub>O.

**Table 2.** The calculated natural atomic charges (e) of TNAZ, H<sub>2</sub>O, complexes **1**, **2**, and **3** at B3LYP/6-311++G\*\* level

Atom	Mono- mer	<b>1</b>	<b>2</b>	<b>3</b>	$\Delta 1^*$	$\Delta 2$	$\Delta 3$
C <sub>1</sub>	-0.18988	-0.18759	-0.18855	-0.19108	0.00229	0.00133	-0.0012
C <sub>2</sub>	0.21506	0.21411	0.21880	0.22292	-0.00095	0.00374	0.00786
C <sub>3</sub>	-0.18991	-0.19389	-0.18339	-0.18758	-0.00398	0.00652	0.00233
N <sub>4</sub>	-0.32614	-0.31373	-0.32765	-0.31583	0.01241	-0.00151	0.01031
N <sub>5</sub>	0.48156	0.48237	0.49354	0.48466	0.00081	0.01198	0.00310
O <sub>6</sub>	-0.31850	-0.31416	-0.32389	-0.33592	0.00434	-0.00539	-0.01742
O <sub>7</sub>	-0.34233	-0.34902	-0.34621	-0.33569	-0.00669	-0.00388	0.00664
N <sub>8</sub>	0.47584	0.47481	0.47790	0.48046	-0.00103	0.00206	0.00462
O <sub>9</sub>	-0.32410	-0.33307	-0.32499	-0.34056	-0.00897	-0.00089	-0.01646
O <sub>10</sub>	-0.33569	-0.32525	-0.35136	-0.32772	0.01044	-0.01567	0.00797
N <sub>11</sub>	0.62293	0.62741	0.62279	0.62618	0.00448	-0.00014	0.00325
O <sub>12</sub>	-0.37818	-0.37448	-0.38280	-0.39830	0.00370	-0.00462	-0.02012
O <sub>13</sub>	-0.37624	-0.41828	-0.37965	-0.38210	-0.04204	-0.00341	-0.00586
H <sub>14</sub>	0.24205	0.24502	0.24552	0.26187	0.00297	0.00347	0.01982
H <sub>15</sub>	0.24972	0.24714	0.24254	0.24228	-0.00258	-0.00718	-0.00744
H <sub>16</sub>	0.23871	0.27260	0.24399	0.23064	0.03389	0.00528	-0.00807
H <sub>17</sub>	0.25511	0.24792	0.25939	0.26292	-0.00719	0.00428	0.00781
O <sub>18</sub>	-0.91272	-0.94677	-0.94445	-0.95329	-0.03405	-0.03173	-0.04057
H <sub>19</sub>	0.45636	0.46592	0.47703	0.47716	0.00956	0.02067	0.02080
H <sub>20</sub>	0.45636	0.47894	0.47144	0.47899	0.02258	0.01508	0.02263

\*  $\Delta 1$ ,  $\Delta 2$  and  $\Delta 3$  show the resulting deviations from the initial atomic charges for complexes **1**, **2** and **3** in (e) respectively.\*\* Atomic numbering from 1 to 17 belongs to TNAZ and that from 18 to 20 belongs to H<sub>2</sub>O.

Table 2 lists the atomic charges of TNAZ, H<sub>2</sub>O and the complexes obtained by NBO analysis. The charge redistribution mainly occurs between the intermolecular contacting atoms of the two submolecules. Table 3 gives the NBO analysis of the donor and the acceptor (bonding-antibonding) between the submolecules and their stabilization energy  $\Delta E$  according to second-order perturbation theory. This was carried out by examining all possible interactions between ‘filled’ (donor) Lewis-type NBOs and ‘empty’ (acceptor) non-Lewis NBOs; the stabilization energies  $\Delta E$  are proportional to the NBO interacting intensities. Table 3 shows that the oxygen atoms in the nitro group donate lone pairs to the neighbouring O–H antibonds belonging to the H<sub>2</sub>O in complex **1**. As opposed to complex **1**, the oxygen in the nitro group in complexes **2** and **3** acts as a moderate hydrogen acceptor. Table 3 also shows that complex **1** has two

large interaction energies, 6.025 and 3.849 kJ/mol, whilst the largest interaction energies for complexes **2** and **3** are 3.138 and 1.927 kJ/mol, respectively. The order of the stabilization energies is **1** > **2** > **3**. Therefore, charge transfer changes occur in an inconsistent fashion with the interaction energy and is not the main factor causing the weak intermolecular interactions in these complexes. The data provided in Table 3 show that the charge transfer between the two subsystems is very small. The dipole moments of TNAZ, H<sub>2</sub>O and complexes **1**, **2** and **3** are 2.1577, 0.5588, 1.7146, 2.5886 and 1.8336 Debye, respectively.

**Table 3.** NBO analysis results for complexes **1**, **2**, and **3** at B3LYP/6-311++G\*\* level

Complex	Donor NBO	Acceptor NBO	$q_{i \rightarrow j}$ /a.u.	$F(i,j)$ /a.u.	$\Delta E$ /(kJ/mol)
<b>1</b>	BD (1)C <sub>3</sub> -H <sub>16</sub>	BD*(1)O <sub>18</sub> -H <sub>19</sub>	$2.768 \times 10^{-04}$	0.012	0.711
	LP(1)O <sub>13</sub>	BD*(1)O <sub>18</sub> -H <sub>19</sub>	$7.692 \times 10^{-05}$	0.008	0.251
	LP(1)O <sub>13</sub>	BD*(1)O <sub>18</sub> -H <sub>20</sub>	$7.512 \times 10^{-04}$	0.025	2.469
	LP(2)O <sub>13</sub>	BD*(1)O <sub>18</sub> -H <sub>19</sub>	$1.611 \times 10^{-04}$	0.007	0.335
	LP(2)O <sub>13</sub>	BD*(1)O <sub>18</sub> -H <sub>20</sub>	$3.159 \times 10^{-03}$	0.031	6.025
	LP(3)O <sub>13</sub>	BD*(1)O <sub>18</sub> -H <sub>20</sub>	$1.676 \times 10^{-03}$	0.022	2.469
	BD(1)O <sub>18</sub> -H <sub>20</sub>	BD*(1)C <sub>3</sub> -N <sub>4</sub>	$7.346 \times 10^{-05}$	0.006	0.209
	LP(2)O <sub>18</sub>	BD*(1)C <sub>2</sub> -C <sub>3</sub>	$3.055 \times 10^{-04}$	0.011	0.759
	LP(2)O <sub>18</sub>	BD*(1)C <sub>3</sub> -N <sub>4</sub>	$9.512 \times 10^{-05}$	0.006	0.251
	LP(2)O <sub>18</sub>	BD*(1)C <sub>3</sub> -H <sub>16</sub>	$1.401 \times 10^{-03}$	0.027	3.849
<b>2</b>	LP(2)O <sub>10</sub>	BD*(1)O <sub>18</sub> -H <sub>19</sub>	$3.287 \times 10^{-04}$	0.010	0.628
	LP(1)O <sub>18</sub>	BD*(1)C <sub>3</sub> -N <sub>4</sub>	$4.354 \times 10^{-04}$	0.009	0.628
	LP(2)O <sub>18</sub>	BD*(1)C <sub>3</sub> -N <sub>4</sub>	$1.336 \times 10^{-03}$	0.023	3.138
<b>3</b>	LP(3)O <sub>7</sub>	RY*(1)O <sub>18</sub>	$2.642 \times 10^{-04}$	0.010	0.418
	LP(3)O <sub>7</sub>	BD*(1)O <sub>18</sub> -H <sub>20</sub>	$2.337 \times 10^{-04}$	0.008	0.335
	LP(1)O <sub>18</sub>	BD*(1)C <sub>1</sub> -H <sub>14</sub>	$9.877 \times 10^{-04}$	0.016	1.925
	LP(2)O <sub>18</sub>	BD*(1)C <sub>1</sub> -H <sub>14</sub>	$6.426 \times 10^{-04}$	0.019	1.757

\*  $\Delta E$  denotes the stabilization energy; **BD** denotes bonding orbital; **BD\*** denotes antibonding orbital; **LP** denotes lone-pair. For BD and BD\*; **(1)** and **(2)** denote  $\sigma$  orbital and  $\pi$  orbital, respectively. For LP: **(1)**, **(2)** denote the first and the second lone pair electrons, respectively; **RY\*** denotes empty orbital out of valence orbital.  $q_{i \rightarrow j}$  denotes amounts of transferred partial charge between a donor and an acceptor species and  $F(i,j)$  denotes the matrix element of Fock operator between donor and acceptor wave functions.

### Interaction energies

The uncorrected and corrected interaction energies including  $\Delta E$ ,  $(\Delta E)_C$  and  $(\Delta E)_{C,ZPE}$  of the complexes are defined by:

$$\Delta E = E_{(\text{TNAZ} + \text{H}_2\text{O})} - (E_{(\text{TNAZ})} + E_{(\text{H}_2\text{O})}) \quad (3)$$

$$(\Delta E)_c = (\Delta E) + \text{BSSE} \quad (4)$$

$$(\Delta E)_{c,ZPE} = (\Delta E)_c + \text{ZPE} \quad (5)$$

where  $(\Delta E)_c$  is the interaction energy corrected with the BSSE correction and  $(\Delta E)_{c,ZPE}$  is corrected with both the BSSE and ZPE corrections.

Table 4 shows the uncorrected and corrected interaction energies of complexes **1**, **2** and **3**. Generally, the energy will decrease when two molecules interact, which is called the interaction energy or binding energy. The stability of the complex is closely related to the interaction energy [17]. The corrected binding energy for complex **3** is -18.49 kJ/mol, which is the largest for all three complexes, and is almost the same as the best experimental estimate for the dissociation energy (approx. 15 kJ/mol) of water dimers [18], indicating that hydrogen bonding in complex **3** is almost as strong as in a water dimer. The binding energy for complex **1**, -14.12 kJ/mol, is the smallest of all the complexes, indicating that the oxygen in the nitro group acts as only a moderate hydrogen acceptor.

**Table 4.** Total energy (E), zero point energy (ZPE) and interaction energy ( $\Delta E$ ) of monomers, complexes **1**, **2**, and **3** at B3LYP/6-311++G\*\* level\* (in kJ/mol)

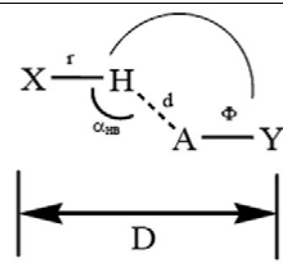
	E	ZPE	$\Delta E$	$(\Delta E)_c$	$(\Delta E)_{c,ZPE}$	BSSE	$(ZPE)_c$
TNAZ	-2066132.39	278.33					
H <sub>2</sub> O	-200741.87	55.87					
<b>1</b>	-2266897.21	340.47	-22.94	-20.14	-14.12	2.82	6.02
<b>2</b>	-2266900.18	340.82	-25.91	-21.03	-14.68	4.86	6.35
<b>3</b>	-2266905.34	341.40	-31.07	-25.41	-18.49	5.64	6.91

According to Table 4, the trend for the uncorrected interaction energies is complex **3** > complex **2** > complex **1**. After the BSSE and the ZPE corrections, the interaction energies of the complexes were in the same order as that for the uncorrected interaction energies. The BSSE of the three complexes are 2.82, 4.86 and 5.64 kJ/mol, respectively, and the corrected ZPE values are 6.02, 6.35 and 6.91 kJ/mol, respectively. This means that it is essential to carry out the BSSE and ZPE corrections. According to the simple hydrogen bond X-H.....A-Y model, where the group X-H is called the donor and A-Y is called the acceptor, the strength of the hydrogen bond is described by geometrical parameters such as d, D,  $\Phi$ , r and  $\alpha_{\text{HB}}$  which are introduced in Table 5. These parameters for complexes **1**, **2**, and **3** have been collected and compared to reference parameters



[19]. Consequently, hydrogen bonding makes an insignificant contribution to the intermolecular interactions in the complexes **1**, **2**, and **3**.

**Table 5.** Calculated values of hydrogen bond parameters for TNAZ/H<sub>2</sub>O complexes **1**, **2**, and **3** at the B3LYP/6-311++G\*\* level



	$r_{\text{mon}}$	$r_{\text{dim}}$	$\Delta r$ (Å)	$d$ (Å)	$\alpha_{\text{HB}}$	$D$ (Å)
<b>1</b>	0.96217	0.96634	0.00417	2.121	144.66	2.962
<b>2</b>	0.96217	0.96386	0.00169	2.445	115.33	2.987
<b>3</b>	0.96217	0.96314	0.00097	2.947	89.40	3.090

### Thermodynamic properties

Based on statistical thermodynamics and vibrational analysis, the thermodynamic functions, including heat capacities ( $C_p$ ), entropies ( $S^0_T$ ), thermal correction to enthalpies ( $H^0_T$ ) and Gibbs free energies ( $\Delta G_T$ ), were calculated by opposing the corrected factor 0.96 [20]; these have been listed in Table 6 for four temperatures (200, 298.15, 500 and 700 K). Both the entropies and the enthalpies decreased during the formation of the complexes from their monomers; it can be predicted that the intermolecular interaction is an exothermic process accompanied by a decrease in the probability of formation. The intermolecular interaction results in the  $C_p$  values of the complexes being larger than the summation of the monomers'  $C_p$ s. For the same temperature, the order  $(\Delta H_T)_3 > (\Delta H_T)_2 > (\Delta H_T)_1$  also gives the same interacting order of **3** > **2** > **1** as derived from the interaction energies. It is not difficult to find that the sequence of  $\Delta G_T$  is the same as that of  $\Delta H_T$ , and that the value of  $\Delta G_T$  increases as the temperature increases, thus the interactions are weakened as the temperature increases. Since the value of  $\Delta H_T$  is less sensitive to temperature than that of  $T\Delta S$ , the effect of temperature upon  $\Delta G_T$  is mainly derived from the contributors to the  $T\Delta S$  term for the same complex. It is energetically and thermodynamically unfavourable for TNAZ to bind with H<sub>2</sub>O and to form any stable complexes at room temperature.

**Table 6.** Thermodynamic properties of TNAZ, H<sub>2</sub>O, complexes **1**, **2**, and **3** at different temperatures

Structure	Temp. (K)	C <sub>P</sub> (J/mol·K)	S <sup>0</sup> <sub>T</sub> (J/mol·K)	H <sup>0</sup> <sub>T</sub> (kJ/mol)	ΔS <sub>T</sub> (J/mol·K)	ΔH <sub>T</sub> (kJ/mol)	ΔG <sub>T</sub> (kJ/mol)
TNAZ	200	130.838	403.409	17.202			
	298.15	172.695	463.445	32.102			
	500	246.538	571.296	74.848			
	700	294.031	662.419	129.277			
H <sub>2</sub> O	200	33.288	186.016	6.650			
	298.15	33.477	194.414	9.924			
	500	35.912	211.472	16.940			
	700	38.640	223.986	24.394			
<b>1</b>	200	130.801	405.681	17.234	-183.74	29.87	66.62
	298.15	218.652	541.188	41.963	-116.67	-16.07	18.71
	500	246.070	573.116	74.709	-209.65	20.18	125.00
	700	296.186	664.453	129.282	-221.95	13.16	168.53
<b>2</b>	200	173.737	443.040	22.301	-146.39	-13.16	16.12
	298.15	219.388	521.034	41.622	-136.83	-18.91	21.89
	500	296.445	653.988	94.208	-128.78	-9.00	55.39
	700	347.243	762.542	159.013	-123.86	-6.19	80.52
<b>3</b>	200	173.172	446.537	22.272	-142.89	-17.58	10.99
	298.15	218.790	524.297	41.549	-133.56	-23.39	16.44
	500	296.445	656.942	94.001	-125.83	-13.59	49.32
	700	346.833	765.329	158.709	-121.08	-10.88	73.88

$$\Delta S_T = [(S^0_T)_{ii} - \sum (S^0_T)_i] \times 0.96; \Delta H_T = [(E_o + H_{corr})_{ii} - \sum (E_o + H_{corr})_i] \times 0.96; \Delta G_T = \Delta H_T - T\Delta S_T$$

(i = TNAZ and H<sub>2</sub>O; ii = **1**, **2** and **3**).

## Conclusions

We can draw the following conclusions from the DFT/B3LYP/6-311++G\*\* calculations:

1. After the BSSE and ZPE corrections, the corrected intermolecular interaction for complex **3** was 18.49 kJ/mol. Therefore, complex **3** is the most stable of the three complexes. The sequence of the stability of the optimized complexes is **3** > **2** > **1**.
2. The charge transfer between the two subsystems is very small. However, charges on the intermolecular contacting atoms and the neighbouring atoms obviously change, but the charge transfers alter in an inconsistent fashion

- with the interaction energy and charge transfer is not the main cause of the weak intermolecular interactions in these complexes.
3. The oxygen atoms of the nitro groups donate lone pairs to neighbouring O-H, C-N and C-H antibonds. The stabilizing energies are proportional to the NBO interaction intensities. The largest interaction energy is 6.025 kJ/mol in complex **1**.
  4. The intermolecular interaction is an exothermic process accompanied by a decrease in the probability of conversion from monomers to complexes. As the temperature increases, the  $\Delta S_T$  and  $\Delta H_T$  values decrease, while the  $\Delta G_T$  value increases; thus, the interactions are weakened as the temperature increases. It is energetically and thermodynamically unfavourable for TNAZ to bind with H<sub>2</sub>O and to form a stable complex at room temperature, based on the  $\Delta G_T$  values.

## References

- [1] Watt D.S., Cliff M.D., *Evaluation of 1,3,3-Trinitroazetidine (TNAZ) – A High Performance Melt-castable Explosive*, DSTO-TR-1000, July **2000**, pp. 1-22.
- [2] Iyer S., Eng Y.S., Yoyee M., Perz R., Alster J., Stock D., *The 11th Annual Working Group, Institute on Synthesis of High Density Materials*, Kiamesha Lakes, **1992**.
- [3] Sikder N., Sikder A.K., Bulakh N.R., Gandhe B.R., 1,3,3-Trinitroazetidine (TNAZ). A Melt-cast Explosive: Synthesis, Characterization and Thermal Behavior, *J. Hazard. Mater.*, **2004**, *113*, 35-43.
- [4] Badgular D.M., Talawar M.B., Asthana S.N., Mahulikar P.P., Advances in Science and Technology of Modern Energetic Materials: An Overview, *J. Hazard. Mater.*, **2008**, *151*, 289-305.
- [5] Sikder A.K., Sikder N., A Review of Advanced High Performance, Insensitive and Thermally Stable Energetic Materials Emerging for Military and Space Applications, *J. Hazard. Mater.*, **2004**, *A112*, 1-15.
- [6] Agrawal J.P., *High Energy Materials: Propellants, Explosives and Pyrotechnics*, WILEY-VCH, **2010**.
- [7] Ju X.H., Xiao H.M., Xia Q.Y., A Density Functional Theory Investigation of 1,1-Diamino-2,2-dinitroethylene Dimers and Crystal, *J. Chem. Phys.*, **2003**, *119*, 10247-10255.
- [8] Chalasinski G., Szczesniak M.M., State-of-the-art and Challenges in the *ab initio* Theory of Intermolecular Interactions, *Chem. Rev.*, **2000**, *100*, 4227-4252.
- [9] Ju X.H., Xiao H.M., Intermolecular Interaction of Hydrazine Dimers: a Comparative Theoretical Study, *J. Mol. Struct. (Theochem)*, **2002**, *588*, 79-86.
- [10] Fletcher R.M., Powell J.D., A Rapidly Converging Descent Method for Minimization, *J. Comput.*, **1963**, *6*, 163-166.

- [11] Schlegel H.B., Optimization of Equilibrium Geometries and Transition States, *J. Comput. Chem.*, **1982**, *3*, 214-218.
- [12] Oftadeh M., Hamadani M., Radhoosh M., Keshavarz M.H., DFT Molecular Orbital Calculations of Initial Step in Decomposition Pathways of TNAZ and some of Its Derivatives with -F, -CN and -OCH<sub>3</sub> Groups, *J. Mol. Struct. (Theochem)*, **2011**, *964*, 262-268.
- [13] Peng C., Ayala P.Y., Schlegel H.B., Frisch M.J., Using Redundant Internal Coordinates to Optimize Equilibrium Geometries and Transition States, *J. Comput. Chem.*, **1996**, *17*, 49-56.
- [14] Sherrill C.D., Counterpoise Correction and Basis Set Superposition Error, <http://vergil.chemistry.gatech.edu/notes/cp.pdf/> (accessed Mar 20, 2010).
- [15] Frisch M.J., Trucks G.W., Schlegel H.B., Scuseria G.E., Robb M.A., Cheeseman J.R., Montgomery J.A., Vreven T., Kudin K.N., Burant J.C., Millam J.M., Iyengar S.S., Tomasi J., Barone V., Mennucci B., Cossi M., Scalmani G., Rega N., Petersson G.A., Nakatsuji H., Hada M., Ehara M., Toyota K., Fukuda R., Hasegawa J., Ishida M., Nakajima T., Honda Y., Kitao O., Nakai H., Klene M., Li X., Knox J.E., Hratchian H.P., Cross J.B., Adamo C., Jaramillo J., Gomperts R., Stratmann R.E., Yazyev O., Austin A.J., Cammi R., Pomelli C., Ochterski J.W., Ayala P.Y., Morokuma K., Voth G.A., Salvador P., Dannenberg J.J., Zakrzewski V.G., Dapprich S., Daniels A.D., Strain M.C., Farkas O., Malick D.K., Rabuck A.D., Raghavachari K., Foresman J.B., Ortiz J.V., Cui Q., Baboul A.G., Clifford S., Cioslowski J., Stefanov B.B., Liu G., Liashenko A., Piskorz P., Komaromi I., Martin R.L., Fox D.J., Keith T., Laham M.A.A., Peng C.Y., Nanayakkara A., Challacombe M., Gill P.M.W., Johnson B., Chen W., Wong M.W., Gonzalez C., GAUSSIAN 03, Pople, Gaussian, Inc.: Pittsburgh, PA, **2003**.
- [16] Reed A.E., Curtiss L.A., Weinhold F., Intermolecular Interactions from a Natural Bond Orbital, Donor-acceptor Viewpoint, *Chem. Rev.*, **1988**, *88*, 899-926.
- [17] Diao K.S., Wang F., Wang H.J., Ab initio Theoretical Study of the Interactions between CFCl<sub>3</sub> and SO<sub>2</sub>, *B. Environ. Contam. Tox.*, **2010**, *84*, 170-174.
- [18] Sun X.-Q., Ju X.H., Xuand H.J., Fan X.W., Theoretical Study on the Intermolecular Interactions between 1,1-Diamino-2,2-dinitroethylene and H<sub>2</sub>O, *J. Chin. Chem. Soc.*, **2007**, *54*, 1451-1456.
- [19] Steiner T., The Hydrogen Bond in the Solid State, *Angew. Chem. Int.*, **2002**, *41*, 48-76.
- [20] Cramer C.J., *Essentials of Computational Chemistry: Theories and Models*, John Wiley & Sons. Ltd, **2004**.